Fickian Ingress of Binary Solvent Mixtures into Glassy Polymer

R. Sackin, E. Ciampi, J. Godward, J. L. Keddie, and P. J. McDonald*

Department of Physics, University of Surrey, Guildford, Surrey, GU2 7XH, UK

Received August 16, 2000

ABSTRACT: The ingress of miscible mixtures of a good and a bad solvent (methyl ethyl ketone and ethanol) into poly(styrene) has been visualized using magnetic resonance imaging (MRI). The use of both ^{2}H imaging with selectively deuterated solvents and $^{13}C-^{1}H$ cyclic cross-polarization (CYCLCROP) chemically selective imaging with normal solvents allows the individual components of the solvent mixtures to be measured separately. The two solvents are found to ingress together. However, the spatial concentration profiles are markedly different. The methyl ethyl ketone profile shows a sharp solvent front at the interface between the swollen rubber and the noninvaded glass and has a high solvent fraction throughout the rubber. The ethanol profile shows that the ethanol fraction decreases smoothly across the rubber and approaches zero at the front. These results are explained in terms of a simple multicomponent diffusion model, wherein the diffusion of the bad solvent is enabled by the presence of the good solvent.

Introduction

The ingress of pure solvents into glassy polymers has been investigated by numerous researchers[1−5] to the extent that the controlling mechanisms are now reasonably well understood. In everyday situations, however, polymers are often exposed to mixtures of solvents. One example is polymer composite in aircraft and cars exposed to mixtures of water and the solvents comprising petroleum. Another is dental resin exposed to water and trace solvents in the mouth.[6] The resulting ingress is of obvious importance but is less well understood than single-component ingress. The manufacturing of industrial asymmetric membranes relies on the mass transfer of good and bad solvents in a glassy polymer. Either a solvent/nonsolvent/polymer ternary mixture or a polymer/solvent binary mixture is exposed to a coagulation bath of nonsolvent. Precipitation times have been shown to be dependent on the ternary diffusion coefficients.[7] It has been highlighted in the literature[8] that the diffusivity of a binary solvent mixture cannot be considered to be the additive sum of its components when they differ in molecular volumes and polarities.

The ingress of solvent mixtures has been measured experimentally by a number of groups. Kwei and Zupko[9] used optical methods to measure binary solvent ingress into cross-linked glassy epoxy polymers. For a mixture of methanol (a bad solvent) and methyl ethyl ketone (a good solvent) they found a single advancing front that progressed with Fickian dynamics. However, they could not distinguish the individual solvent component concentrations in the swelling sample. Miller et al.[10] studied mixtures of 2-propanol with varying proportions of toluene, benzene, acetone, and carbon tetrachloride ingressing into poly(carbonate). They inferred from subsequent gas chromatography experiments that 2-propanol, which, unlike the other solvents, does not cause stress cracking, was not sorbed. In other work, van der Zeeuw et al.[11] have assumed that when a miscible solution of methyl ethyl ketone and water is in contact with poly(styrene), the water, which is a bad solvent for the polymer, does not enter the polymer at all. In stark contrast to this assumption, Cooper et al.[8] observed binary mixtures of methyl ethyl ketone and alcohols with various chain lengths ingressing poly(methyl methacrylate) (PMMA) and found that a small amount of kinetically good (i.e., small molecular size) but thermodynamically bad solvent mixed with a kinetically bad but thermodynamically good solvent increased the polymer dissolution rate. They concluded that smaller nonsolvent molecules diffuse *ahead* of larger good solvent molecules, thereby increasing the dissolution rate. Manjikow et al.[12] observed similar results for other systems.

Webb and Hall[13] studied Fickian diffusion of two solvents in rubbery polymers using magnetic resonance imaging (MRI) techniques. Chemical shift selection enabled them to observe the solvent components independently. For the system of benzene and acetone ingressing vulcanized rubber, they found that the ingress rates of the two components when mixed were identical and intermediate between the two pure component rates. However, they made no assessment of the solvent concentration profiles of the two components within the swelling polymer. In further work, Webb and Hall[14] placed vulcanized rubber in a reservoir containing a mixture of water and acetone. An NMR spectrum of the sample recorded after 2 weeks of solvent exposure showed that only acetone had ingressed the polymer. Last, Lane et al.[15] used MRI to show that a small quantity of acetone could induce a transition between Fickian and linear case II[16,17] ingress for methanol diffusion into PMMA.

The short review above leads to the conclusion that the understanding of the ingress of mixed solvents into glassy polymers is far from complete. It is particularly unclear whether a bad solvent will diffuse ahead of, alongside, or behind a miscible good solvent. The issues raised highlight the need for spatially resolved and solvent-specific concentration data. The availability of this kind of data is extremely limited. It is the purpose of this paper to explore the separate concentration profiles of binary mixtures of miscible good and bad solvents ingressing a glassy polymer. We chose to study the system of a miscible mixture of methyl ethyl ketone

* To whom correspondence should be addressed.

10.1021/ma001442y CCC: $20.00
Published on Web 01/16/2001

and ethanol ingressing glassy poly(styrene). This system is chosen first because the molecular size of the good solvent (methyl ethyl ketone) is larger than that of the bad solvent (ethanol) and second because it exhibits Fickian behavior as opposed to more complicated case II behavior. Measurements are made using ^{1}H MRI,[18] ^{2}H MR profiling, and chemically selective ^{13}C−^{1}H cyclic cross-polarization MR profiling techniques. The ^{2}H and cross-polarization methods allow separate mapping of the two solvents in the swollen polymer. A simple model is described that reproduces the essential features of the experimental data.

Samples and Methods

The poly(styrene) of molecular weight $M_n = 3.14 \times 10^5$ g/mol and polydispersity (M_w/M_n) of 1.04 was obtained as a powder from Polymer Laboratories (UK). It was pressed into small cylindrical pellets at 50 kN m^{-2} and 180 °C for 8 h in a vacuum and slowly cooled to room temperature still under vacuum. The pellets were 8 mm in diameter and 4 mm long. Once formed, they were pushed into close-fitting cylindrical poly(tetrafluoroethylene) sleeves open at one end. The use of these sleeves ensured that the solvent ingress was unidirectional, as was confirmed by two-dimensional ^{1}H magnetic resonance microscopy measurements. The sleeved pellets were immersed in liquid solvent within the imaging magnet. The volume of liquid far exceeded that of polymer, so that it could be considered to be an infinite reservoir. The HPLC-grade solvents, methyl ethyl ketone (MEK) and ethanol (EtOH), were obtained from Sigma-Aldrich (UK). In some experiments, one of the solvents in the mixture was deuterated, and ^{2}H MR profiling was used so as to separately visualize the MEK or EtOH component. For this purpose $CH_3CD_2COCD_3$ and CD_3-CH_2OH were also purchased.

For ^{1}H magnetic resonance imaging measurements, carried out at 400 MHz, a standard two-dimensional Fourier transform imaging sequence was used[18] with the following experimental parameters: echo time, 14.5 ms; maximum phase gradient and read gradient strengths, 2.45 and 9.79 G/cm, respectively; and repetition time, 1 s. The chosen slice width was typically 1 or 2 mm, and 512 and 128 read points and phase encode steps, respectively, were used. After standard Fourier data processing, the resulting in-plane image pixel size was 23 μm by 94 μm. However, the true resolution was somewhat less. Images, with data averaging, were typically recorded in 20 min. In the case of ^{1}H MRI, one-dimensional profiles were extracted from the central region of the image data. The two-dimensional measurement with slice selection was preferred over direct one-dimensional profiling as it was possible to verify that the sample was swelling uniformly and that there was minimal swelling distortion. For ^{2}H experiments, the gradient strengths and NMR frequency were adjusted in accordance with the change in the gyromagnetic ratio of ^{1}H and ^{2}H. Moreover, for the most part, only one-dimensional profiles were acquired in order to maintain an adequate data signal-to-noise ratio in a comparable data acquisition time.

The two different solvents could not both be seen separately in the same sample. Such a separation would have required quasi-simultaneous ^{1}H and ^{2}H measurements with one solvent fully deuterated. To overcome this limitation, and thereby image both solvents sequentially in the same sample, ^{13}C-edited chemically resolved images were obtained using cyclic cross-polarization methods (CYCLCROP), described in detail elsewhere.[19] With CYCLCROP, all the ^{1}H signal is excited. The magnetization of a particular chemical subspecies—here the CH_3 linked to the CH_2 of the MEK or the CH_3 of the EtOH—is then selectively transferred to ^{13}C for storage while the remaining ^{1}H magnetization is destroyed. The stored ^{13}C magnetization is then returned to the ^{1}H and imaged as usual. In this manner, chemical specific images are obtained. In the CYCLCROP experiments reported here, the PRAWN variant of the method[20] was used with 15 coupling pulses of nominal flip angle 24° applied over 4.5 ms. The ^{13}C was naturally abundant, and profiles typically took 2.4 h to acquire. They were not therefore acquired during the early part of the ingress when the concentrations were varying rapidly.

All the magnetic resonance images and profiles showed the region of swollen polymer and solvent solution. The signal intensity was, however, variably attenuated by nuclear spin relaxation and self-diffusion. Nonetheless, a distinct rubber/glass interface could be resolved. The spin−spin relaxation time of the nuclei in the polymer glass was too short for this region to be seen.

To assess the spin−spin relaxation times of the solvents in the polymer, a series of equilibrated mixtures of MEK, EtOH, and poly(styrene) were prepared. The MEK concentration ranged from 10 to 40 wt %, and the EtOH concentration ranged from 2.5 to 10 wt %. The samples were made by adding known quantities of the solvents to poly(styrene) in NMR tubes which were then cooled in liquid nitrogen prior to sealing under vacuum. The samples were equilibrated for 48 h at 80 °C before the ^{1}H relaxation times of the individual components were measured using the Carr−Purcell−Meiboom−Gill (CPMG) sequence weighted NMR spectroscopy.

In passing, we comment on the use of conventional magnetic resonance microscopy with an echo time of 14.5 ms rather than conventional microscopy with a shorter echo time or indeed rather than a broad line technique, such as stray field imaging (STRAFI) (with an echo time as little as 50 μs), which we have used elsewhere.[15] While it is possible to measure quantitatively the polymer solvent volume fractions at low solvent fractions using relaxation contrast in STRAFI, since all components are quantitatively reflected in the measurement, the separation is technically difficult at higher fractions. At higher fractions the T_2* of the mobile solvent is reduced by diffusion in the strong field gradient to values comparable to that of the increasingly mobile polymer. Conventional microscopy with a shorter echo time, on the other hand, introduces a significant (but not quantified) polymer signal into the image. As with many NMR techniques, a compromise is required.

Experimental Results

We consider first the equilibrated samples of poly(styrene) in mixed solvents. In general, samples in which the weight ratio of MEK:EtOH exceeded 4:1 did not form a homogeneous phase but phase-separated into a two-phase mixture that was optically opaque. When the MEK weight fraction in the sample exceeded about 20 wt %, narrow spectral lines were resolved, and the EtOH and MEK relaxation times were both very long. For example, well above the glass transition at a composition of 68.0 wt % poly(styrene), 25.7 wt % MEK, and 6.3 wt % EtOH, the T_2 of the MEK methyl groups is measured at 2.54 s, and the T_2 of the EtOH methyl group is 3.43 s. Spectra representative of those from which these values are calculated are shown in Figure 1a. Both values are substantially longer than the imaging echo time (14.5 ms) so that, for this composition, the solvent signals will be insignificantly attenuated by T_2 relaxation in ^{1}H images. The poly(styrene) shows only as a broad baseline to the spectrum and is therefore not seen in the images. At lower MEK fraction (<20 wt %) the lines broadened somewhat, making it more difficult to clearly resolve the MEK and EtOH. The broadened lines represent reduced T_2 of both MEK and EtOH. For example, Figure 1b shows representative spectra recorded close to the glass transition at a composition of 78.1 wt % poly(styrene), 18.9 wt % MEK, and 3.0 wt % EtOH. The methyl group T_2 values measured from these and other spectra are 25 ms (MEK) and 57 ms (EtOH). These are still longer than the image echo time so that, although the solvent signals close to the glass transition will be attenuated

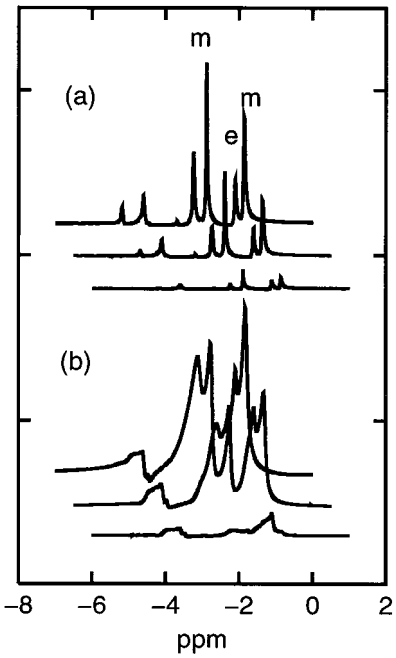

Figure 1. (a) Representative CPMG weighted spectra obtained from an equilibrated solution with a PS:MEK:EtOH weight ratio of 68.0:25.7:6.3. The spectra shown (from the top) are recorded after relaxation weighting delays of 0.02, 1.6, and 6.0 s. The two MEK methyl group lines and the one EtOH methyl group line used to measure T_2 are labeled *m* and *e*, respectively. The spectra are offset one from the next to aid viewing. (b) As in (a), but for delays of 1, 10, and 100 ms and PS:MEK:EtOH ratios of 78.1:18.9:3.0. The OH line of EtOH is not seen.

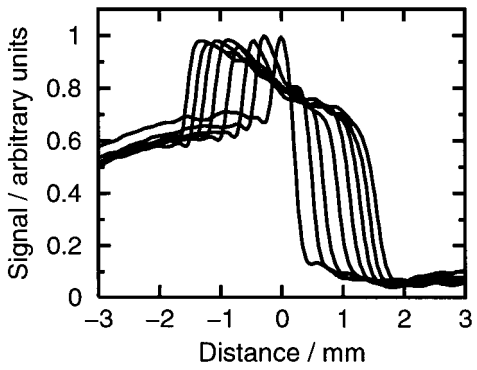

Figure 2. ^{1}H profiles of a 80 wt % methyl ethyl ketone/20 wt % ethanol mixture ingressing into poly(styrene) recorded at 2 h intervals. The solvent is to the left, the progressively swelling rubber is in the center, and the glass is to the right. The original sample surface is at 0 mm on the scale.

by T_2 relaxation in ^{1}H images, both solvents will be seen. Importantly for the conclusions discussed below, the MEK signal will be more attenuated than the EtOH signal.

We now consider the spatially resolved ingress data. Figure 2 shows typical ^{1}H profiles extracted from spin-echo images of poly(styrene) exposed to a binary mixture of 80 wt % MEK and 20 wt % EtOH in a liquid reservoir, with those shown being recorded at 2 h intervals. The central part of each profile shows signal from the swollen rubber region of the sample. With time, this region is seen to swell. The solvent reservoir is to the left. The signal from the reservoir is strongly attenuated by rapid self-diffusion of the liquid molecules in the magnetic field gradient and by the short repetition time of the experiment compared to the free liquid nuclear

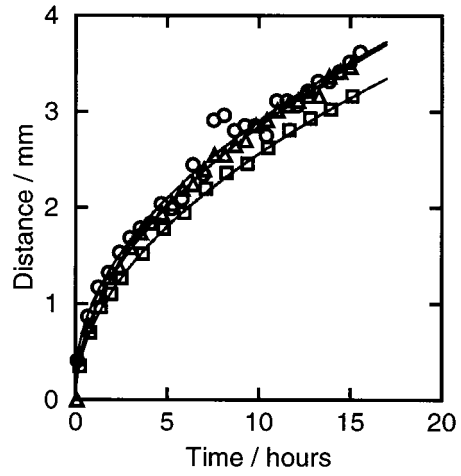

Figure 3. Width of the rubber region in swelling poly(styrene) exposed to a 80 wt % methyl ethyl ketone/20 wt % ethanol mixture recorded using ^{1}H (squares), ^{2}H methyl ethyl ketone (circles), and ^{2}H ethanol (triangles) profiling. The solid lines are fits to the equation $z = At^{1/2}$. The solvent fronts go in together. For clarity, only alternate data points are shown.

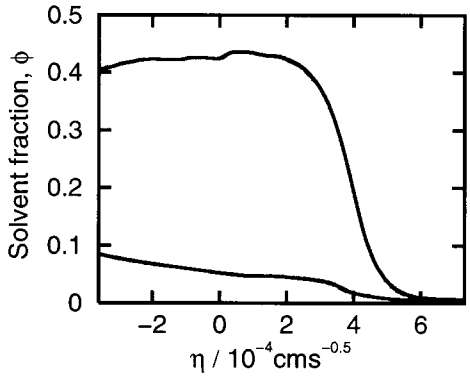

Figure 4. ^{2}H Boltzmann-transformed master curves of 80 wt % methyl ethyl ketone (top line) and 20 wt % ethanol (bottom) in a mixture ingressing poly(styrene).

spin−lattice relaxation time. The polymer glass (not visualized) is to the right. The width of the rubber region has been directly measured from these and other profiles and is shown in Figure 3. It is clear that the polymer swelling is in accordance with generalized Fickian diffusion since the width increases with the square root of time. No evidence was found, either in the profiles or from subsequent NMR spectroscopy of the solution above the polymer sample, for polymer dissolution when the solvent reservoir contained 20 wt % EtOH and 80 wt % MEK.

To assess whether both solvents are ingressing together, Figure 4 shows ^{2}H profiles recorded in two further experiments in which one or the other of the solvents was partially deuterated. The profiles have been transformed according to the Boltzmann transform,[21] $\eta = z/2t^{1/2}$, where t is time and z is position, and are therefore presented in the form of a master experimental profile. Use of the Boltzmann transform means that profiles recorded at different times can be directly compared. The MEK master profile is calculated from 69 individual data profiles and the EtOH master profile from 53 data profiles. The intensities of the two profiles presented in Figure 4 have been normalized such that the rubber surface concentration of each solvent is set equal to the equilibrium concentration. These latter values were determined from quantitative NMR spec-

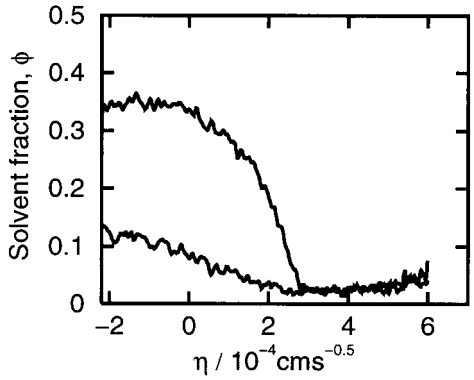

Figure 5. Cyclic cross-polarization $^{13}C-^{1}H$ chemically edited Boltzmann transformed master curves of 70 wt % methyl ethyl ketone (top line) and 30 wt % ethanol (bottom line) in a mixture ingressing poly(styrene).

troscopy of equilibrated swollen samples. Figure 5 shows comparable results using $^{13}C-^{1}H$ cyclic cross-polarization chemical-edited natural abundance ^{13}C profiling of MEK and EtOH except that, in this case, a slightly lower MEK fraction (70%) and higher EtOH fraction (30%) was used so as to slow the ingress. The results are presented in a similar format. Importantly, these master curves are constructed from multiple profiles recorded sequentially from a single sample. Each master profile is calculated from 10 data profiles. From both the ^{2}H and $^{13}C-^{1}H$ experiments, it is clear that both solvents ingress the polymer. Moreover, the MEK and EtOH solvent fronts are coincident within experimental error, as is shown in Figure 3 (circles and triangles) despite the fact that the MEK is a good solvent and the EtOH is a bad solvent for the poly(styrene). The width of the rubber region in the ^{2}H data is systematically slightly larger than in the corresponding ^{1}H data. The most likely reason is that the ^{2}H experiments required larger imaging-gradient-current strengths which slightly warmed the probe and sample.

The basic result, that the MEK and EtOH fronts move in together, was also discovered for mixtures of acetone and methanol ingressing PMMA.[22] It is, however, counter to the conclusions of Miller et al.[10] and the assumptions of van der Zeeuw et al.[11] and Manjikow et al.[12] but is consistent with some of the experimental results obtained for ingress into vulcanized rubber by Webb and Hall.[13,14]

Although the MEK and EtOH fronts move in together, there is strong evidence in both the ^{2}H and $^{13}C-^{1}H$ results that the concentration profiles of the two solvents in the swollen region are different. Since the spin−spin relaxation times of the MEK and EtOH are comparable at any given location within the rubber, we conclude that the MEK concentration profile is significantly more square than the corresponding EtOH profile. In particular, the MEK shows a sharp interface at the rubber−glass transition while the EtOH does not. The EtOH concentration profile varies only slowly across the rubber, and the interface is much less distinct. In practice, at lower solvent fractions close to the interface between the rubber and the glass, where T_2 attenuation starts to have an impact, the MEK T_2 (albeit measured only for ^{1}H) is shorter than that of the EtOH. Hence, the MEK signal is attenuated by T_2 more than the EtOH signal. This serves only to accentuate the differences in the solvent profile shapes highlighted above in the region of the interface. This observation of different profile shapes is a significant new result which requires further explanation.

Analysis

Various attempts have been made to explain mixed solvent diffusion in polymers beginning with the work of Cussler and Lightfoot.[23] More recently, Devotta and Mashelkar[24] have presented a model, in part to explain the unexpected dissolution behavior in some systems already discussed,[8,12] which predicts that, in general, competition between thermodynamic and kinetic factors will lead to differential solvent uptake rates. They predict that smaller bad solvent molecules will diffuse ahead of larger good solvent molecules. However, their model—the test of which was the original driving force for this particular study—cannot explain our results since it neglects coupling between the three components in the diffusion problem.

We prefer to build on the earlier ideas of Cussler and Lightfoot.[23] For a ternary multicomponent diffusion system such as this, one can write[25]

$$F_i = -\sum_{j=1}^{3} D_{i,j} \frac{\partial \phi_j}{\partial z} \tag{1}$$

where F_i is the flux of component i, $D_{i,j}$ is a multicomponent diffusion coefficient, ϕ_j is the concentration of component j, and z is position measured from the solvent−polymer interface. In general, $D_{i,j} \neq D_{j,i}$ and the coefficients are strongly concentration-dependent. Conservation of mass and total flux means that only four of the nine components $D_{i,j}$ are mutually independent. For systems such as dilute gases, the equations can be reformulated in terms of the pairwise binary diffusion coefficients $D^{*}_{i,j}$. However, for condensed liquids and polymers this is not so straightforward. Some authors[26] develop the analysis in terms of chemical potential driving forces and Flory−Huggins theory.[27] Such analysis is attractive from the viewpoint of trying to characterize fully the ingress. However, it suffers in that it relies on adequate models of the chemical potential in the nonequilibrium swelling polymer and on models of the mobilities of the different components, both of which are difficult to obtain. Moreover, the approach then requires a larger number of fit parameters with which to apply the model. We base our analysis on a model derived from pairwise exchange of components as might be used in a simple Monte Carlo calculation.

According to this very much simpler model, we write

$$F_i = \frac{D^{+}_{i,j}}{\sum_k \phi_k}\left(\phi_i \frac{\partial \phi_j}{\partial z} - \phi_j \frac{\partial \phi_i}{\partial z}\right) \tag{2}$$

and hence

$$\frac{\partial \phi_i}{\partial t} = \frac{1}{\sum_k \phi_k}\left[\sum_{i \neq j}\left(\frac{\partial}{\partial z} D^{+}_{i,j}\left(\phi_j \frac{\partial \phi_i}{\partial z} - \phi_i \frac{\partial \phi_j}{\partial z}\right)\right)\right] \tag{3}$$

where $D^{+}_{i,j}$ are an alternate (but related) set of diffusion coefficients. The number of independent parameters is now reduced to three since, in a model based on exchange, we require $D^{+}_{i,j} = D^{+}_{j,i}$. The set of diffusion

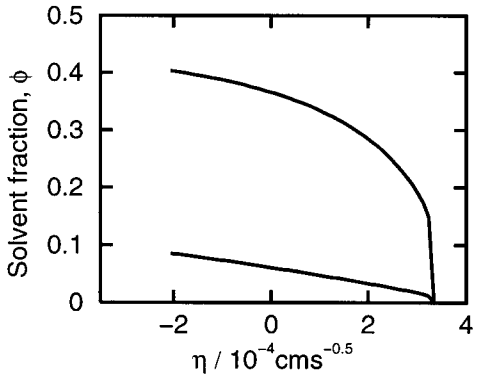

Figure 6. Theoretical master curves of methyl ethyl ketone (top line) and ethanol (bottom). Values of parameters are given in the text. The methyl ethyl ketone profile shows a sharp front with a high solvent fraction throughout the rubber. The ethanol fraction decreases across the rubber to near zero at the interface with the glass. These simulated profiles compare favorably with the experimental data in Figure 5, in particular.

equations are solved numerically for the boundary conditions,

$$\phi_i = \phi_i^{eq} \qquad z = 0,\ t \geq 0$$

$$\phi_i = 0 \qquad z > 0,\ t = 0,\ i = \text{MEK, EtOH}$$

$$\phi_i = 1 \qquad z > 0,\ t = 0,\ i = \text{PS} \tag{4}$$

The first condition states that the surface of the sample is maintained at equilibrium concentration throughout. The second states that the interior of the sample is initially pure polymer. The characteristic features of the data now result if we assume the following diffusivities:

$$D^+_{\text{MEK,EtOH}} = \text{constant}$$

$$D^+_{\text{MEK,PS}} = \text{constant},$$

$$\phi_{\text{MEK}}/(\phi_{\text{MEK}} + \phi_{\text{PS}}) \geq \phi_{\text{TG}} \text{ else } D^+_{\text{MEK,PS}} = 0$$

$$D^+_{\text{EtOH,PS}} = 0 \tag{5}$$

The first of these equations describes a single, concentration-independent mutual diffusivity for the two solvents. The second describes a strongly concentration-dependent diffusivity for MEK in poly(styrene). The simplest possible form is chosen: a step function. The critical concentration, ϕ_{TG}, is the MEK fraction in poly(styrene) (PS) required to induce a glass-to-rubber transition at the experimental temperature and is of the order of 0.15. The last states that EtOH does not diffuse in poly(styrene).

Figure 6 shows the resultant theoretical, Boltzmann-transformed master profiles in which due allowance has been made for the swelling of the polymer. The theoretical profiles should be compared directly to the experimental data in Figures 4 and 5. An overlay is not attempted, since the experimental data are weighted by nuclear spin relaxation attenuation as discussed above. Nonetheless, the essential features are seen. The key point is that the solvent fronts move together, but the shapes of the concentration profiles are very different. The MEK shows a sharp solvent front, whereas the EtOH concentration varies much more uniformly. The MEK front arises because of the strong concentration dependence of $D^+_{\text{MEK,PS}}$. However, since the flux at the solvent front is not limited by the viscoelastic polymer swelling, the system is Fickian, not case II.[1] The EtOH cannot proceed beyond the front but can diffuse rapidly in the swollen region in the presence of the MEK. The flux of EtOH across the swollen region, which is proportional to the concentration gradient, matches that required to keep pace with the swelling of the polymer by the ingressing MEK. In consequence, the EtOH concentration at the glass/rubber interface remains constant and small.

The values of diffusion coefficients used in this simulation are $D^+_{\text{MEK,EtOH}} = 1 \times 10^{-9}$ m^2 s^{-1} and $D^+_{\text{MEK,PS}} = 1 \times 10^{-9}$ m^2 s^{-1} for $\phi_{\text{MEK}}/(\phi_{\text{MEK}} + \phi_{\text{PS}}) > \phi_{\text{TG}} = 0.17$. These values of diffusion coefficient are consistent with experimentally measured diffusion coefficients resulting from direct integration of the Boltzmann transformed experimental data.The value of $D^+_{\text{MEK,EtOH}}$ is also consistent with typical values for the diffusion coefficient of small molecules to be found in the literature,[28] and $D^+_{\text{MEK,PS}}$ for larger concentrations is consistent with values reported for small molecules in swollen polymers.[2−5] The diffusion coefficients of both MEK at low concentration and EtOH in the glass are expected to be very small. The surface concentrations of MEK and EtOH in the swollen rubber, ϕ_{MEK} and ϕ_{EtOH}, were set equal to 0.40 and 0.09, respectively. These surface concentrations have been estimated by comparison of NMR spectra of equilibrated mixtures formed from poly(styrene) exposed to a large solvent reservoir and spectra of the reservoir. The values are consistent with expectation based on Flory−Huggins theory[27] with the three interaction parameters: $\chi_{\text{MEK-EtOH}}$, $\chi_{\text{MEK-PS}}$, and $\chi_{\text{EtOH-PS}}$ set to 0.0, 0.5, and 1.5, respectively.

Conclusions

We have obtained the first data that provide separate spatially resolved concentrations of the components of mixtures of good and bad solvents ingressing into a glassy polymer. For the system studied, methyl ethyl ketone and ethanol ingressing poly(styrene), the two solvents ingress simultaneously, with neither solvent ingressing ahead or behind the other. However, the concentration profiles appear rather different. The good solvent exhibits a strong solvent concentration front, whereas the bad solvent concentration varies smoothly and slowly across the swollen region. The effects can be explained in terms of a simple model wherein the bad solvent diffuses within the swollen rubber only by virtue of the presence of the good solvent.

Acknowledgment. The authors thank the UK Engineering and Physical Science Research Council for financial support (Grant GR/M 00268). R.S. thanks the same council for a research studentship. E.C. thanks Unilever Research for financial support. The authors thank Drs. David Faux and Richard Sear (University of Surrey) for useful discussions.

References and Notes

(1) Thomas, N. L.; Windle, A. H. *Polymer* **1982**, *23*, 529.
(2) Mills, P. J.; Palmstrom, C. J.; Kramer, E. J. *J. Mater. Sci.* **1986**, *21*, 1479.
(3) Weisenberger, L. A.; Koenig, J. L. *Macromolecules* **1990**, *23*, 2445.
(4) Hyde, T. M.; Gladden, L. F.; Mackley, M. R.; Gao, P. *J. Polym Sci., Polym. Chem.* **1995**, *33*, 1795.
(5) Hassan, M. M.; Durning, C. J. *J. Polym. Sci., Part B: Polym. Phys.* **1999**, *37*, 3159.
(6) Scrimgeour, S. N.; Lloyd, C. H.; Hunter, G.; Lane, D. M.; McDonald, P. J. In *Spatially Resolved Magnetic Resonance*;

Blümler, P., Blümich, B., Botto, R., Fukushima, E., Eds.; Wiley-VCH: Weinheim, Germany, 1998.
(7) Tsay, C. S.; McHugh, A. J. *J. Polym. Sci., Part B: Polym. Phys.* **1990**, *28*, 1327.
(8) Cooper, W. J.; Krasicky, P. D.; Rodriguez, F. *J. Appl. Polym. Sci.* **1986**, *31*, 65.
(9) Kwei, T. K.; Zupko, H. M. *J. Polym. Sci., Part A2* **1969**, *7*, 867.
(10) Miller, G. W.; Visser, S. A. D.; Morecroft, A. S. *Polym. Eng. Sci.* **1971**, *11*, 73.
(11) van der Zeeuw, E. A.; Sagis, L. M. C.; Koper, G. J. M. *Macromolecules* **1996**, *29*, 801.
(12) Manjikow, J.; Papanu, J. S.; Soong, D. S.; Hess, D. W.; Bell, A. T. *J. Appl. Phys.* **1987**, *62*, 682.
(13) Webb, A. G.; Hall, L. D. *Polymer* **1991**, *32*, 2926.
(14) Webb, A. G.; Hall, L. D. *Polym. Commun.* **1990**, *31*, 425.
(15) Lane, D. M.; McDonald, P. J.; Keddie, J. L. In *Spatially Resolved Magnetic Resonance*; Blümler, P., Blümich, B., Botto, R., Fukushima, E., Eds.; Wiley-VCH: Weinheim, Germany, 1998.
(16) Alfrey, T. *Chem. Eng. News* **1965**, *43*, 64.
(17) Thomas, N. L.; Windle, A. H. *Polymer* **1982**, *23*, 529.
(18) Callaghan, P. *Principles of Nuclear Magnetic Resonance Microscopy*; Oxford University Press: Oxford, UK, 1991.
(19) Heidenreich, M.; Köckenberger, W.; Kimmich, R.; Chandrakumar, N.; Bowtell, R. *J. Magn. Reson.* **1998**, *132*, 109.
(20) Heidenreich, M.; Spyros, A.; Köckenberger, W.; Chandrakumar, N.; Bowtell, R.; Kimmich, R. In *Spatially Resolved Magnetic Resonance*; Blümler, P., Blümich, B., Botto, R., Fukushima, E., Eds.; Wiley-VCH: Weinheim, Germany, 1998.
(21) Crank, J. *The Mathematics of Diffusion*; Oxford University Press: Oxford, UK, 1975.
(22) McDonald, P. J.; Heidenreich, M.; Kimmich, R., unpublished results.
(23) Cussler, E. L.; Lightfoot, E. N. *J. Phys. Chem.* **1965**, *69*, 1135.
(24) Devotta, I.; Mashelkar, R. A. *Chem. Eng. Commun.* **1996**, *156*, 31.
(25) Bird, R. B.; Stewart, W. E.; Lightfoot, E. N. *Transport Phenomena*; Wiley: New York, 1960.
(26) Bindschaedler, C.; Gurny, R.; Doelker, E.; Peppas, N. A. *J. Colloid Interface Sci.* **1985**, *108*, 75.
(27) Flory, P. J. *Principles of Polymer Chemistry*; Cornell University Press: Ithaca, NY, 1953.
(28) Weast, R. C. *CRC Handbook of Chemistry and Physics*, 67th ed.; CRC Press: Boca Raton, FL, 1986.

MA001442Y